A study on monitoring multi-scale concrete members with coda-wave interferometry using embedded transducers

Chapter · March 2021

DOI: 10.1201/9780429279119-330

CITATIONS
0

READS
43

5 authors, including:

Yuguang Yang
Delft University of Technology
49 PUBLICATIONS **272** CITATIONS

SEE PROFILE

Bridge Maintenance, Safety, Management, Life-Cycle Sustainability and Innovations – Yokota & Frangopol (eds)

A study on monitoring multi-scale concrete members with coda-wave interferometry using embedded transducers

C. Kevinly, F. Zhang, Y. Yang, D. Draganov & C. Weemstra
Delft University of Technology, Delft, The Netherlands

ABSTRACT: This paper presents a study on the application of the coda-wave interferometry (CWI) technique using embedded transducers for the monitoring of concrete structural members. The coda-wave interferometry (CWI) has been recognized as a promising technique in detecting small changes in the parameters of materials. To reduce the influence of environment and enable the access to the interested region of the target structure we propose to apply CWI with embedded transducers for the monitoring concrete structures. In this paper, the proposed approach is applied on a 0.5-m cylinder under compression and on a 10-m full-scale beam under bending. The results showed a good correspondence between the CWI-deducted wavespeed change and the estimated strain value in both the small-scale and the large-scale test. Besides, the correlation coefficient of the coda, especially the late coda is sensitive to the formation of cracks even at a distance from the sensor pair. Thus, they can be used as crack indicators of the structure.

1 INTRODUCTION

The concept of monitoring concrete structures with ultrasonic waves have been explored for decades (Naik T.R. 1991, Tomoki Shiotani 2009, Hashimoto et al. 2017, Zhang et al. 2018). One of the main challenges is that the concrete is a heterogeneous material, and most of its damages have similar or smaller dimensions compared to the scatterers (aggregates). However, recent research has revealed that the multiply scattered ultrasonic waves, generally referred to as "coda", turn out to be an effective tool to measure small changes in the bulk material with a technique called coda-wave interferometry (CWI) originally proposed in geosciences, the technique is sensitive to parameters such as stresses (Stähler et al. 2011), temperature (Larose et al. 2006), and mechanical damages (Schurr et al. 2011). Therefore, studies on applying CWI for monitoring concrete structures is increasing rapidly recently (Planès and Larose 2013).

In a separate development, to bring the measurements close to the region of interest, and at the same time obtain a stable coupling between the sensors and the structure, embedded piezo-electric-based transducers (Smart Aggregates) are used as sources and sensors (Song et al. 2008, Du et al. 2018). The combination of both technologies, therefore, may provide a promising solution for the monitoring of both new and existing concrete structures.

In this paper, we present a preliminary study on applying CWI with embedded transducers for monitoring of concrete structures. The research is carried out with tests at two different scales: a 0.5-m concrete cylinder, and a 10-m full-scale concrete beam. Compression tests and shear tests were applied on the cylinders and the beam, respectively. During the tests, the CWI was applied using a stretching technique to find the wavespeed change. Comparing to the estimated strain from displacement measurements, the performance of CWI on the indication of strain change is evaluated. The results of this research give insight on the reliability of CWI using embedded sensors for monitoring multiple scaled concrete members

2 THEORY

Though the multiply scattered waves are complex, they were found to be sensitive for minor changes in the medium (Wapenaar and Snieder 2007). The changes of the arrival time of the coda over time (equivalent to wavespeed change) can be quantified using a stretching technique (Stähler et al. 2011). The altered 'stressed' signal is stretched in the time domain to fit the 'baseline' signal by searching the highest correlation coefficients.

DOI: 10.1201/9780429279119-330
https://doi.org/10.1201/9780429279119-330

$$CC(\varepsilon) = \frac{\int_{t_1}^{t_2} h^{(stressed)}[t(1-\varepsilon)]h^{(baseline)}[t]dt}{\sqrt{\int_{t_1}^{t_2}\left(h^{(stressed)}\right)^2[t(1-\varepsilon)]dt}\sqrt{\int_{t_1}^{t_2}\left(h^{(baseline)}\right)^2[t]dt}} \quad (1)$$

where ε is the wavespeed change (also expressed as dv/v), t_1 and t_2 are the start and end times of the window applied to both the 'stressed' wave $h^{(stressed)}$ and the baseline $h^{(baseline)}$, and CC is the correlation coefficient or 'degree of similarity' between the coda of the 'stressed' wave and the coda of the baseline.

The correlation coefficient is computed for a set of ε values. The value of ε' for which $CC(\varepsilon)$ reaches the maximum is the wavespeed change between the coda of the 'stressed' wave and the coda of the baseline. A positive/negative ε' implies that the coda of the 'stressed' wave is compressed/stretched and arrives earlier/later than the coda of the baseline. They can be related to the deformation of the medium.

To be able to include the late coda of the signal, which has relatively low amplitude, a windowing operation was made to the signals with rectangular windows. The described stretching calculation was made on windowed signals.

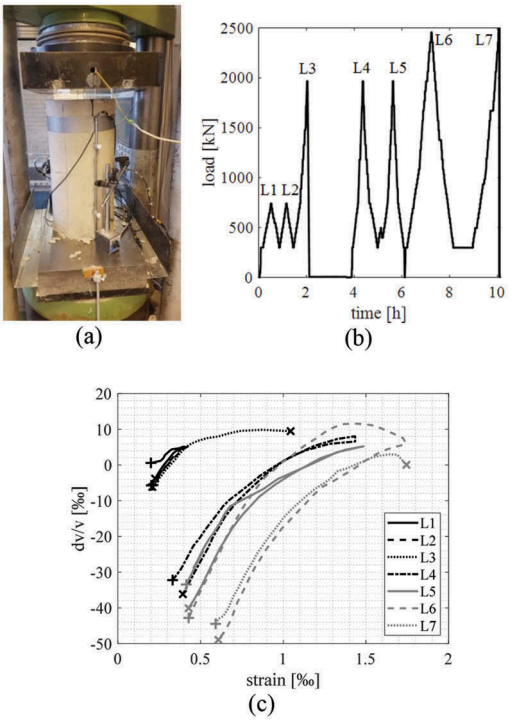

Figure 1. (a) Cylinder specimen test setup, (b) loading history, (c) wavespeed change with strain.

3 INFLUENCE OF STRESS LEVEL ON WAVE SPEED IN A CYLINDER TEST

A concrete cylinder with a diameter of 250 mm and a height of 480 mm was subjected to compressive cyclic loading (Figure 1a). The concrete has a nominal compressive strength of 65 MPa. The maximum aggregate size is 16 mm. Two smart aggregates (SA) with a central frequency of 88 kHz were embedded inside the specimen with a center to center distance of 250 mm in the loading direction. They act as signal source and receiver respectively. The specimen is loaded by uniaxial compression with cyclic loading procedure as is indicated in Figure 1b, with the load cycles numbered from L1 to L7. The longitudinal (axial) deformation of the cylinder was measured by two LVDTs at both sides.

During the test, the loading procedure was divided by small load steps. At every load step, repeated single sinus bursts with a frequency of 88 kHz was sent to the source SA transducer. The CWI analysis was applied on the signal recorded by the receiver SA transducer. Ten windows of 90 μs (around eight times the source wave period) were selected from the first arrival with an overlap of 50% between consecutive windows. The wave speed change was searched by stretching technique in each window. Only the windows with a maximum correlation coefficient above 0.8 were selected as reliable windows. The mean value of the wavespeed changes of all the reliable windows was used as the output of the analysis.

The cylinder sample failed at around 2500 kN. Major permanent deformation was observed at the end of the load cycle L3, along with spalling on the specimen. The wavespeed change was compared to the average strain measured by LVDT, see Figure 1c. The marker '+' indicates the start, and the marker '×' indicates the end of a load cycle. It shows that the wavespeed positively correlated to the compressive strain. The gradient of the curves decreased as the load level increased, a similar observation was also made in terms of the wavespeed change vs. stress (Stähler et al. 2011). In the repeated load cycles, the wavespeed – strain curve seems to be quite consistent with certain amount reduction in terms of wave speed during the unloading process of each load cycle. Both observations could be attributed to the propagation of micro cracks. When the maximum load that is applied on the cylinder is significantly higher than the previous load cycle, a clear drop of the wavespeed was observed, such examples can be found in the loading branches of L4 and L6. These drops of waves speed could be related to the development of internal damage (macro cracks) inside the specimen.

4 INFLUENCE OF STRESS DISTRIBUTION TO WAVE SPEED IN A BEAM TEST

To explore the possibility of applying the monitoring technique on real structural members, a test on a reinforced concrete beam with dimensions of 10 m × 1.2 m × 0.3 m was carried out. The specimen was simply supported with support distance of 9 m and loaded by a point load at 3 m from one support, see Figure 2. The same type of concrete was used. The tensile reinforcement of the beam was 8Ø25 mm plain bars. Five SA transducers were embedded in the upper part of the beam, and thirteen Acoustic Emission (AE) transducers were installed on one side of the surface covering the total height of the beam. The AE transducers were R6I-AST (MISTRAS 2008), with a central frequency of around 60 kHz. LVDTs were installed on the same surface to measure the displacement.

The loading procedure is shown in Figure 3a, which included five load levels: 100 kN, 150 kN, 200 kN, 250 kN, and 300 kN. In each load level, three load cycles were applied, except for the last load level, when shear failure occurred in the second load cycle. In the first load cycle in each load level, small load steps of 10 kN or 20 kN were set to allow the active measurement of wavespeed with the SA transducers. In this test, SA4 was used and the source transducer, while the other SA transducers were used as receivers.

The result from the transducer pair SA4-SA5 are located in the compression zone with similar distance as in the cylinder test. Thus the measurement of the transducer pair was employed to compared with the study of concrete cylinder. Similarly a LVDT was installed on the side surface of the beam to estimate the average strain between the SA pair. The results

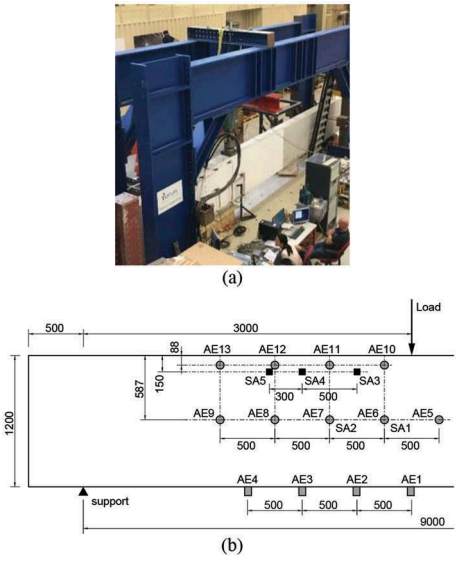

Figure 2. Beam specimen: (a) Test setup, (b) Sensor layout.

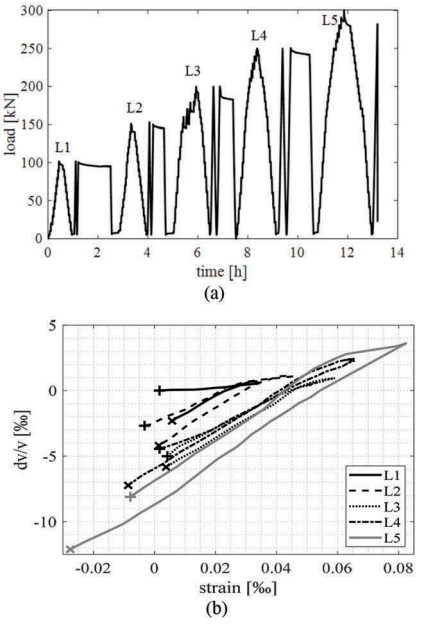

Figure 3. Beam-specimen tests: (a) Loading history, (b) wavespeed change vs strain.

are given in Figure 3b. The marker '+' indicates the start, and the marker '×' indicates the end of a load cycle. In the figure, similar observations as the concrete cylinders can be made. However, because that the maximum strain in the concrete compression zone was less than 0.08‰, the relationship between wavespeed change and strain was more linear. Since the load steps were small, even with the strain change of around 0.001‰ can be detected. However, the wavespeed change includes the effect elastic deformation and the propagation of micro cracks. It is still unclear how to separate these two effects. By the end of the last load level, a significant drop of wavespeed was observed accompanied by an increase of tensile strain. This was due to the shear crack which initiated from the bottom and ended near the ray path SA4-SA5 (see Figure 7).

The comparison between the cylinder test and beam test presented above suggested a consistent performance. An increase of wavespeed was observed in both tests when the concrete medium had a compressive strain. However, the slope of the wavespeed-to-compressive-strain curve was not quantitatively comparable. The ratio between the wavespeed change and strain was around 55 for the cylinder under compression and around 152 for the beam under bending. This may due to the different strain distribution in the near field, the aggregates, and the boundary conditions.

In addition to single SA pair, an attempt was made to extend the measurement wave speed change to the whole shear zone of the beam. To do so, the embedded SA transducers were combined with externally installed AE transducers to form an extended sensor

network. When the beam was fully loaded and unloaded, the SA transducers were used as signal source one after another, while the other SA transducers and all the AE sensors were used as receiver. For each load level, the same signal-processing method was applied using the baseline signals obtained in the unloaded condition before the first cycle, and stressed signal obtained in the loaded condition at the third load cycle when the beam was fully loaded.

The results of the full-scale measurements at L2 is illustrated in Figure 4, where the increase of wavespeed is indicated in blue, while decrease – in red. The intensity of the color represents the magnitude of the change. Transducer AE4 were not included due to the poor coupling to the surface of the beam. This shows the benefit of using permanent embedded sensors where the coupling between the sensor and the specimen is more reliable. The figure shows a clear transition from reduction of wave speed to increase, while no significant change of wavespeed was measured along the central line of the beam. Note that at L2, the maximum load level was 150 kN. According to a previous calculation, the maximum tensile stress of the beam was still less that the tensile strength of concrete, thus the beam still behaved linear-elastically without any major crack. From Figure 4, one may conclude that the distribution of the wavespeed reflects reasonably the strain (stress) distribution of the beam under single point load. The opening of the first crack occurred at around 175 kN. After that, the correlation of the signals in the cracked area became poor (with a maximum correlation coefficient lower than 0.6) and led to unreliable wavespeed-change estimates.

5 EFFECT OF CRACKING TO THE WAVE SIGNAL COHERENCE IN A BEAM TEST

The stretching technique (Stähler et al. 2011) applied in the study works under the condition that the travelling path of the multiscattered wave is stable. That ensures the signal after stretching comparable to the based line signal, which is reflected by the coherence of the wave signal, the *CC* (Correlation Coefficient). Therefore, the value of *CC* could be used to evaluate the reliability of the resultant ε. In our calculation, the calculated ε based on the windows with CC value lower than 0.7 are discarded, to ensure a reliable result.

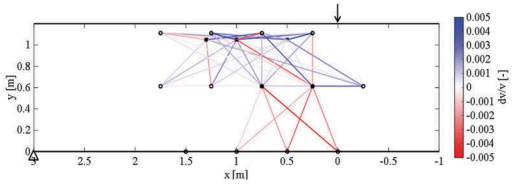

Figure 4. Wavespeed change at load level 150 kN compared to the unloaded condition.

On the other hand, when the travel path of the coda changes significantly, a clear reduction of *CC* is expected. Such situation may occur when a new crack forms in the medium. Thus, the *CC* level of the coda could be used to investigate the cracking activities of the structure. To demonstrate this effect, the wave signal obtained in the beam test is further investigated by the *CC* value.

In the beam test, to check the relativity of the obtained wavespeed change, the *CC* value of the coda obtained by two sensor pairs, namely SA1-SA4 and SA4-SA5, are given in Figure 5 and 6. As the stretching calculation was made on windowed signal, the *CC* value varies per window. Thus, they are plotted at four representative windows (window 5, 10, 20 and 30) in Figure 5 and 6. The starting times of the four windows and the approximated scattering distance of the signals are listed in Table 1.

For the given sensor pairs, the CC value shown in Figure 5 and 6 suggests that in most steps, the CC values between two adjacent steps are rather close to 1.0 based on the four chosen windows. That suggests

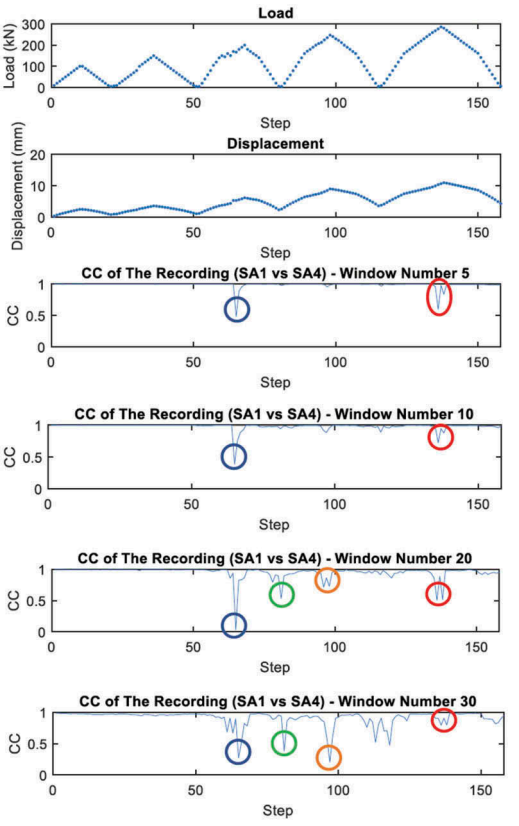

Figure 5. Comparison amonst load, displacement (maximum deflection) and CC of SA1-SA4 sensor pair over load steps. The circles represents the formation of a major crack (see Figure 7 for the color code).

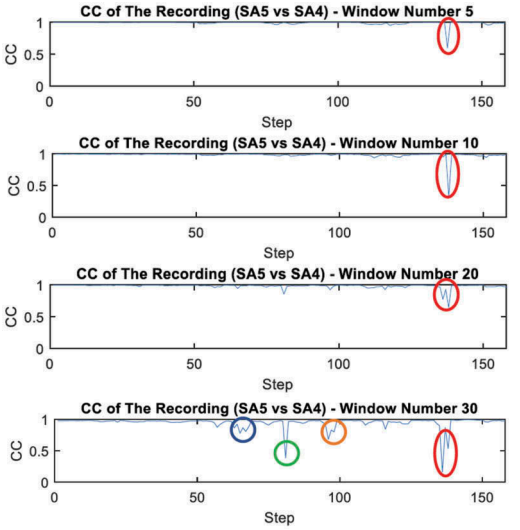

Figure 6. CC of SA1-SA4 sensor pair over load steps. The circles represents the formation of a major crack (see Figure 7 for the color code).

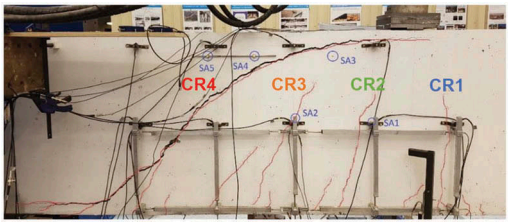

Figure 7. Locations of SA with respect to the final crack pattern.

Table 1. Definition of the referred windows and the corresponding scattering distances.

Window No.	Starting time [ms]	Scattering distance [m]
5	220.5	1
10	447.8	2
20	902.4	4
30	1357.1	6

that the obtained wavespeed changes are reliable at the first instance.

Nevertheless, a number of valleys can be distinguished at several load steps. A further investigation on these load steps showed that they correspond to the formation of major flexural cracks on the beam. Those valleys of *CC* are marked with circles of different colors in Figure 5 and 6. The color code of the corresponding crack is indicated in Figure 7 together with the locations of the SAs.

The comparison suggests that the *CC* value of the coda, especially the late coda is very sensitive to the disturbance of the scattering wave travelling paths, in this case the formation of cracks. In the case of SA1-SA4 pair, Crack 1 – 4 are either across the direct wave path or adjacent to one of the sensor. Therefore, the formation of these cracks are reflected in the *CC* value obtained by window 20 and 30. Among others Crack 1 and 4 are observed in all the windows. Even for the sensor pair SA4 – SA5, although they are not adjacent to Crack 1 – 3, the formation of these cracks are reflected by valley of *CC* of the late coda (window 30), which has a scattering length of 6 m.

The study suggests that the *CC* value of different part of the signal turns out to be a rather sensitive indicator to the formation of cracks inside the concrete structure. Before the application of more advanced inversion techniques, it is not possible to localize the actual position of the cracks. Nevertheless, the windows starting time can still provide an impression on the distance of the crack with respect to the corresponding sensor pair.

6 CONCLUSIONS

We studied the performance of the coda-wave interferometry (CWI) using a new type of embedded transducers smart aggregate (SA) in monitoring the deformation concrete members with different scale.

The measurements were performed on a 0.5-m concrete cylinder under compression and a 10-m full-scale beam. The results in both tests showed a positive correlation between the principal strain of the member and the wavespeed change. In our study, the detectable strain changes were of the order of magnitude of 0.001 ‰. The conclusion can be extended to the full-scale measurements, by combining the embedded transducers with surface transducers, we showed that the technique is able to obtain the elastic deformation in both compression and tension zone of the member.

The study also demonstrated that the technique is sensitive to the cracking of concrete. The formation of micro cracks is considered as the reason of the reduction of the wavespeed after a repeated load cycle for a specimen under uniaxial compression. Upon the formation of a macro crack, the coherence of the coda may be influenced significantly. This was observed in both tests. Therefore, one should be careful with existing concrete structures with cracks already present.

We did not explore the quantitative relationship between the wavespeed change and the strain. This relationship can be influence by many aspects such as: the propagation of micro/macro cracks, the stress distribution, the geometry of the specimens etc. In order to further extend this technology, more study on this topic is called for.

REFERENCES

Du, C., Yang Y. and Hordijk D. 2018. Experimental investigation on crack detection using imbedded smart aggregate. *IALCCE 2018*. Ghent.

Hashimoto, K., Shiotani T., Nishida T. and Miyagawa T. 2017. Application of Elastic-Wave Tomography to Repair Inspection in Deteriorated Concrete Structures. *Journal of Disaster Research* 12: 496–505.

Larose, E., J. de Rosny, L. Margerin, D. Anache, P. Gouedard, M. Campillo and B. van Tiggelen (2006). "Observation of multiple scattering of kHz vibrations in a concrete structure and application to monitoring weak changes." Physical Review E **73**(1): 016609.

MISTRAS 2008. R6I-AST Sensor, PHYSICAL ACOUSTICS CORPORATION..

Naik T.R., M. V. M. 1991. The ultrasonic pulse velocity method. *CRC handbook on nondestructive testing of concrete*, CRC Press: 169–188.

Planès, T. and Larose E. 2013. A review of ultrasonic Coda Wave Interferometry in concrete. *Cement and Concrete Research* 53: 248–255.

Schurr, D. P., Kim J.-Y., Sabra K. G. and Jacobs L. J. 2011. Damage detection in concrete using coda wave interferometry. *NDT & E International* 44(8): 728–735.

Song, G., Gu H. and Mo Y.-L. 2008. Smart aggregates: multi-functional sensors for concrete structures—a tutorial and a review. *Smart materials and structures* 17(3): 033001.

Stähler, S. C., Sens-Schönfelder C. and Niederleithinger E. 2011. Monitoring stress changes in a concrete bridge with coda wave interferometry. *The Journal of the Acoustical Society of America* 129(4): 1945–1952.

Tomoki Shiotani, D. G. A., Osamu Makishima 2009. Global Monitoring of Large Concrete Structures Using Acoustic Emission and Ultrasonic Techniques: Case Study. *Journal of Bridge Engineering*: 2.

Wapenaar, K. and Snieder R. 2007. From order to disorder to order: a philosophical view on seismic interferometry. *SEG Technical Program Expanded Abstracts 2007, Society of Exploration Geophysicists*: 2683–2687.

Zhang, F., Yang Y., Hashimoto K. and Shiotani T. 2018. A comparative study of acoustic emission tomography and digital image correlation measurement on a reinforced concrete beam. *IALCCE 2018*. Ghent.